

**STUDY OF THE REDOX AND ACID-BASE  
PROPERTIES OF SODA-LIME SILICATE GLASS:  
APPLICATION TO THE HIGH TEMPERATURE  
CORROSION OF NICKEL-BASED ALLOYS AND  
CERAMIC MATERIALS**

**TUTI KATRINA BINTI ABDULLAH**

**UNIVERSITI SAINS MALAYSIA**

**2014**

**STUDY OF THE REDOX AND ACID-BASE  
PROPERTIES OF SODA-LIME SILICATE GLASS:  
APPLICATION TO THE HIGH TEMPERATURE  
CORROSION OF NICKEL-BASED ALLOYS AND  
CERAMIC MATERIALS**

**by**

**TUTI KATRINA BINTI ABDULLAH**

**Thesis submitted in fulfillment of the  
requirements for the degree  
of Doctor of Philosophy**

**FEBRUARY 2014**

## **DECLARATION**

I Hereby declare that I have conducted, completed the research work and written the dissertation entitled "Study of the Redox and Acid-Base Properties of Soda-Lime Silicate Glass: Application to the High Temperature Corrosion of Nickel-Based Alloys and Ceramic Materials". I also declare that it has not been previously submitted for the award for any degree or diploma or other similar title of this for any other examining body or University.

Signature:

Candidate's Name: TUTI KATRINA BINTI ABDULLAH

Date:

Signature:

Supervisor's Name: ASSOCIATE PROFESSOR DR. ZUHAILAWATI BINTI

HUSSAIN

Date:

## ACKNOWLEDGEMENTS

Foremost, I would like to thank to my supervisors and co-supervisors from Université de Lorraine (UL) and Universiti Sains Malaysia (USM), Prof. Michel Vilasi (UL), Prof. Christophe Rapin (UL), Assoc. Prof. Dr. Zuhailawati Hussain (USM) and Assoc. Prof. Dr. Afidah Abdul Rahim (USM) for their continuous guidance, patience, motivation and support throughout this study.

My sincere gratitude to Ministry of Education (Malaysia) and USM for granting me the scholarship through Academic Staff Training Scheme (ASTS). My sincere appreciation also goes to Institut Jean Lamour (France) for the financial support during the last few months of my stay in France.

I offer my sincerest gratitude to Dr. Pierre-Jean Panteix and Dr. Carine Petitjean who has supported me throughout this research with their knowledge and patience. All their encouragements and supports help me a lot to complete my study.

I would like to express my gratitude to my fellow lab mates in Corrosion and Thermodynamic Department for the stimulating discussions and for all the time that we had spent for the last four years. A lot of thanks to Lionel and Thierry for always trying to solve my problems.

Last but not least special thanks goes to my family for trusting and allowing me to go abroad for doing my research. I would like to thank to my husband, Annuar Fakry and my daughter, Iman for their encouragement and spiritually support.

## TABLE OF CONTENTS

ACKNOWLEDGEMENTS	iii
TABLE OF CONTENTS	iv
LIST OF TABLES	x
LIST OF FIGURES	xiii
LIST OF SYMBOLS	xxiv
LIST OF ABBREVIATIONS	xxvi
ABSTRAK	xxvii
ABSTRACT	xxix
RÉSUMÉ (FRENCH)	xxxii
<b>CHAPTER 1: INTRODUCTION</b>	<b>1</b>
<b>CHAPTER 2: LITERATURE REVIEW</b>	<b>5</b>
Introduction	5
2.1. General aspects of glass	5
2.1.1. Formation and structure of silicate network	6
2.1.1.1. Network formers	9
2.1.1.2. Network modifiers	9
2.1.1.3. Intermediates	10
2.1.1.4. The role of CaO	11
2.1.1.5. The role of Al <sub>2</sub> O <sub>3</sub>	12
2.1.2. Acid-base properties in glass melts	12

2.1.2.1. Acid-base concepts in glass melts	13
2.1.2.2. Evaluation of acid-base properties in molten glass	16
2.1.2.3. Optical basicity	25
2.1.2.4. Influence of the acid-base properties of the melts on the solubility of oxides	27
2.1.3. Redox properties in silicate melts	28
2.1.3.1. Equilibrium constant	29
2.1.3.2. Redox properties by electrochemical measurement	32
2.2. Corrosion of metals and alloys by molten glass	34
2.2.1. Corrosion of pure metals in molten glasses	34
2.2.1.1. Case of noble metal	35
2.2.1.2. Case of metals used in glass and nuclear industries	37
2.2.2. Corrosion of alloys in molten glasses	41
2.2.2.1. Chromia forming alloys in molten glasses	43
2.2.2.2. Alumina forming alloys in molten glasses	45
2.3. Solubility of important oxides in molten glasses	46
2.3.1 Physicochemical behaviour of chromium oxide in molten glass	48
Summary	54
<b>CHAPTER 3: MATERIALS AND EXPERIMENTAL METHODS</b>	<b>56</b>
Introduction	56
3.1. Raw materials	56
3.1.1. Metal and alloys	56
3.1.1.1. Pure chromium	56
3.1.1.2. Ni-based alloys	57

3.1.2. Glass synthesis	60
3.2. Experimental procedures	63
3.2.1. Corrosion by molten glasses	63
3.2.1.1. Preparation of electrodes	63
3.2.1.2. Electrochemical measurements	68
3.2.1.3. 'Raw immersion' technique	73
3.2.1.4. Thickness loss measurement	75
3.2.2. Solubility of chromia ( $\text{Cr}_2\text{O}_3$ ) in molten glasses	75
3.2.2.1. Glass balls (samples) preparation	75
3.2.2.2. Control of the experimental parameters	76
3.3. Sample characterisation	79
3.3.1. Metallographic preparation	79
3.3.2. Technique of analysis	80
3.3.2.1. Thermogravimetric analysis (TGA)	80
3.3.2.2. X-ray diffraction (XRD) analysis	81
3.3.2.3. Differential thermal analysis (DTA)	81
3.3.2.4. Optical microscope	81
3.3.2.5. Scanning electron microscope (SEM)	81
3.3.2.6. Electron probe micro-analysis (EPMA)	82
<b>CHAPTER 4: CORROSION OF CHROMIA FORMING AND ALUMINA</b>	
<b>FORMING ALLOYS BY MOLTEN GLASSES</b>	<b>83</b>
Introduction	83
4.1. Corrosion of pure Cr and Ni-30Cr by molten glass	84
4.1.1. Electrochemical characterisation of the solvents	85

4.1.2. Electrochemical measurements of the corrosion of pure Cr and Ni-30Cr alloy in silicate melts	88
4.1.2.1 Spontaneous behaviour of pure Cr and Ni-30Cr alloy in NC3S at 1100°C	89
4.1.2.2. Behaviour of preoxidised pure Cr and Ni-30Cr alloy in NC3S at 1100°C	97
4.1.2.3. Influence of temperature on the stability of the passivity states	104
4.1.2.4. Influence of melt basicity on the corrosion behaviour of pure Cr and Ni-30Cr alloy	108
4.1.3. Summary of the behaviour of chromia forming alloys in molten glass media	123
4.2. Corrosion of NiAl and Ni-8Al-28Cr by molten glass	125
4.2.1. Electrochemical measurements of the corrosion of NiAl and Ni-8Al-28Cr alloys in silicate melt	125
4.2.1.1. Spontaneous behaviour of NiAl and Ni-8Al-28Cr alloys in NC3S at 1100°C	125
4.2.1.2. Behaviour of preoxidised NiAl and Ni-8Al-28Cr alloys in NC3S at 1100°C	134
4.2.2. Summary of the behaviour of alumina forming alloys in molten glass media	142

**CHAPTER 5: KINETICS AND THERMODYNAMIC APPROACH OF  
CHROMIA SOLUBILITY IN SILICATE MELTS** **144**



Introduction	144
5.1. Dissolution kinetics of Cr <sub>2</sub> O <sub>3</sub> in the Na <sub>2</sub> O-CaO-xSiO <sub>2</sub> (NCxS) system	145
5.1.1. Influence of oxygen fugacity ( $f_{O_2}$ )	147
5.1.1.1. Oxidising condition (air)	147
5.1.1.2. Reducing condition (Fe/FeO)	154
5.1.2. Influence of temperature	159
5.1.2.1. Oxidising condition (air)	160
5.1.2.2. Reducing condition (Fe/FeO)	163
5.1.3. Influence of melt compositions	165
5.1.3.1. Influence of melt basicity in soda-lime silicate melts	166
5.1.3.2. Influence of oxide modifiers	169
5.1.4. Diffusion of oxygen in the melt	172
5.1.5. Summary of the dissolution kinetics of Cr <sub>2</sub> O <sub>3</sub> in melts	177
5.2. Chromia solubility in silicate melts: Thermodynamic approach	178
5.2.1. Influence of different experimental parameters on the solubility of chromia in silicate melts	179
5.2.1.1. Influence of temperature	179
5.2.1.2. Influence of oxygen fugacity ( $f_{O_2}$ )	181
5.2.1.3. Influence of glass compositions	183
5.2.2. Redox behaviour in silicate melts	191
5.2.2.1. Determination of redox ratio	191
5.2.2.2. Influence of oxygen fugacity ( $f_{O_2}$ ) on Cr redox behaviour in silicate melts	193
5.2.3. Summary of the thermodynamic approach of Cr <sub>2</sub> O <sub>3</sub> in silicate melts	195

5.3. Chromia solubility in soda-lime silicate glass: Correlation with the corrosion of chromia forming alloy in the melt	197
<b>CHAPTER 6: CONCLUSIONS AND FUTURE RESEARCH</b>	
<b>RECOMMENDATIONS</b>	<b>200</b>
<b>REFERENCES</b>	<b>207</b>
<b>APPENDICES</b>	<b>220</b>
Appendix A: Characterisation of the alloys prepared by high frequency induction melting	220
Appendix B: Characterisation of the alloys prepared by pack cementation technique	223
Appendix C: Characterisation of glass precipitates by differential thermal analysis (DTA)	225
Appendix D: Isothermal oxidation of Ni-based alloys	232
<b>LIST OF PUBLICATIONS</b>	<b>244</b>

## LIST OF TABLES

		<b>Page</b>
<b>Table 2.1</b>	The field strength of various cations	8
<b>Table 2.2</b>	The values of $A_{\text{Sun}}$ allowing to determine the acid-base properties of the glass	17
<b>Table 2.3</b>	Optical basicity of oxides determined by Duffy and Ingram	26
<b>Table 2.4</b>	Solubility limit for refractory oxides in soda-lime glass	46
<b>Table 3.1</b>	The elements used as starting materials	57
<b>Table 3.2</b>	The powders used as starting materials	60
<b>Table 3.3</b>	Chemical compositions (theoretical and experimental in wt.%) of soda-lime silicate glasses used in this study	62
<b>Table 4.1</b>	The main corrosion data concerning the spontaneous behaviour of pure Cr and Ni-30Cr alloy in NC3S at 1100°C	96
<b>Table 4.2</b>	Evolution of oxide ( $\text{Cr}_2\text{O}_3$ ) thickness layer formed at the interface pure Cr and Ni-30Cr alloy after 2 h of preoxidation in air at different temperatures	98
<b>Table 4.3</b>	The main corrosion data concerning the corrosion of the preoxidised Ni-30Cr alloy after the immersion in NC3S for two different temperatures	108
<b>Table 4.4</b>	The values of theoretical optical basicity ( $\Lambda_{\text{th}}$ ) and activity of $\text{Na}_2\text{O}$ ( $a_{\text{Na}_2\text{O}}$ ) for binary and ternary silicate melts	109

<b>Table 4.5</b>	The thickness of Cr <sub>2</sub> O <sub>3</sub> layer and the Cr content at the glass/oxide layer interface after 24 h of immersion of preoxidised pure Cr in three different melt compositions at 1050°C	112
<b>Table 4.6</b>	The main corrosion data concerning the corrosion of the preoxidised pure Cr after the immersion un three different melt compositions at 1050°C	114
<b>Table 4.7</b>	Electrochemical characteristics of Ni-30Cr alloy extracted from the I = f(E) curves	117
<b>Table 4.8</b>	Cr solubility (at.% Cr) in soda silicate melts and soda-lime silicate melts at 1200°C in oxidising atmosphere (air)	119
<b>Table 4.9</b>	The thickness of Cr <sub>2</sub> O <sub>3</sub> layer and the Cr concentration measured at the glass/oxide layer interface after 24 h of immersion of preoxidised Ni-30Cr in two different melt compositions at 1050°C	121
<b>Table 4.10</b>	The main corrosion data concerning the corrosion of the preoxidised Ni-30Cr alloy after the immersion in two different melt compositions at 1100°C	122
<b>Table 4.11</b>	Thickness of the alumina layer formed after 2 h and 24 h of preoxidation in air for Ni-8Al-28Cr alloy at 1100°C	134
<b>Table 4.12</b>	Al <sub>2</sub> O <sub>3</sub> solubility in ternary glasses at 1200°C	141
<b>Table 5.1</b>	The physical properties of the studied glass at 1300°C	166
<b>Table 5.2</b>	The physical properties of the studied glass at 1200°C	169
<b>Table 5.3</b>	The experimental data of Cr solubility of NC <sub>x</sub> S (x = 3, 4, 5 and 6) for different temperatures (T = 1200°C, 1300°C and 1350°C) and different oxygen fugacity (-12 ≤ log fO <sub>2</sub> ≤ -0.6)	179

<b>Table 5.4</b>	The activation energy ( $E_a$ ) determined from an Arrhenius plot (Figure 5.23) for different $fO_2$	181
<b>Table 5.5</b>	The values of theoretical optical basicity ( $\Lambda_{th}$ ) for soda-lime silicate melts	184
<b>Table 5.6</b>	The values of theoretical optical basicity ( $\Lambda_{th}$ ) and activity of $Na_2O$ ( $p_a(Na_2O)$ ) at $1200^\circ C$ for soda-lime silicate melts	186
<b>Table 5.7</b>	A comparison between the Cr concentration (at.%) determined in the corrosion study and the limit of Cr solubility which is determined from the thermodynamic study	197

## LIST OF FIGURES

		<b>Page</b>
<b>Figure 2.1</b>	Schematic of two dimensions of (a) crystalline quartz (b) amorphous silica (c) soda silicate glass. The fourth Si-O bond is placed perpendicularly to the plane of the figure	7
<b>Figure 2.2</b>	Schematic of the breaking of Si-O bonding by introducing a Na <sub>2</sub> O molecule in the silicate network	10
<b>Figure 2.3</b>	Log solubility of amphoteric oxides as a function of melt basicity (pO <sup>2-</sup> )	27
<b>Figure 2.4</b>	Compilation of solubility of several oxides in fused pure Na <sub>2</sub> SO <sub>4</sub> at 1200K	28
<b>Figure 2.5</b>	Scale potential used for prediction of corrosion in silicate glasses between 1000°C - 1300°C	34
<b>Figure 2.6(a)</b>	Pt sample immersed in a waste glass containing TeO <sub>2</sub> under argon atmosphere	36
<b>Figure 2.6(b)</b>	Higher magnification of the micrograph of Pt-Te eutectic grain boundary	36
<b>Figure 2.7</b>	Binary phase diagram of Pt-Si	37
<b>Figure 2.8(a)</b>	SEM micrograph of a zirconium plate immersed in G-Fe glass (borosilicate glass containing iron oxide) at 1418°C for 13 h	39
<b>Figure 2.8(b)</b>	The corrosion layers formed are determined by the phase diagram of Zr-Si-O-(Fe-B). The diffusion path is shown by the arrows	39

<b>Figure 2.9</b>	Anodic polarisation of Cr, Fe, Co, and Ni at 1050°C in an industrial soda-lime silicate glass	40
<b>Figure 2.10</b>	$E_{\text{corr}}$ and $R_p$ of preoxidised pure Cr immersed in G-S glass as a function of temperature	41
<b>Figure 2.11</b>	Oxide map for the ternary system Ni-Al-Cr at 1000°C	42
<b>Figure 2.12</b>	Anodic polarisation curves of Co-based alloy in borosilicate glass for active and passive states at 1050°C with scan rate, $v = 10$ mV/min. The interpretation of the curves is supported by the SEM micrographs for both conditions	44
<b>Figure 2.13</b>	Schematic of the $\text{Cr}_2\text{O}_3$ dissolution and redox reactions in molten glass	48
<b>Figure 2.14</b>	Total Cr contents reported as a function of $\log f\text{O}_2$ for four different glass compositions at 1125°C	51
<b>Figure 2.15</b>	Plots of $\log (R_{\text{red}})$ (a) and $\log (R_{\text{ox}})$ (b) determined in the $\text{Na}_2\text{O}-2\text{SiO}_2$ system as a function of $\log f\text{O}_2$ for different temperatures. The obtained equations of the lines are in agreement with the theoretical equations: $\log (R_{\text{red}}) = -0.25 \log f\text{O}_2 + C$ and $\log (R_{\text{ox}}) = 0.75 \log f\text{O}_2 + C$ for reducing and oxidising conditions respectively	54
<b>Figure 3.1</b>	High frequency induction system. (a) upper part (b) lower part	58
<b>Figure 3.2</b>	Schematic of pack cementation which was performed in a silica tube	59
<b>Figure 3.3</b>	Reference electrode (yttria-stabilised zirconia electrode) used in the electrochemical study (a) side view (b) top view	64

<b>Figure 3.4</b>	Schematic of the interfaces of platinum, zirconia and molten glass	64
<b>Figure 3.5</b>	Schematic of a counter electrode (a) side view (b) top view	66
<b>Figure 3.6</b>	Schematic of a working electrode for an electrochemical characterisation of molten glasses (a) side view (b) top view	67
<b>Figure 3.7</b>	Schematic of a working electrode for the corrosion characterisation of metal and alloys (a) side view (b) top view	68
<b>Figure 3.8</b>	Apparatus used for an electrochemical measurements at high temperatures (a) full overview (b) schematic of the furnace and electrodes	69
<b>Figure 3.9</b>	The sample embedded in resin for metallographic preparation	71
<b>Figure 3.10</b>	Schematic of the 'raw immersion' techniques performed on the alloys	74
<b>Figure 3.11</b>	Schematic of a closed system which allows to control simultaneously the different experimental parameters (temperature, basicity (melt composition) and oxygen fugacity ( $fO_2$ ))	76
<b>Figure 3.12</b>	The values of $fO_2$ for the $MO_x/MO_y$ buffers as a function of temperature	78
<b>Figure 4.1</b>	Electroactivity domains of NC3S, NC6S and N2S at 1100°C measured on the Pt working electrode with $v = 1$ mV/s. The potentials are reported with respect to the potential of yttria-stabilised zirconia reference (YSZ) electrode	86



<b>Figure 4.2</b>	Micrographs of pure Cr after 24 h of immersion in NC3S at 1100°C with magnification of (a) 100x and (b) 500x	89
<b>Figure 4.3</b>	Anodic polarisation curve of pure Cr after ~ 40 min of immersion in NC3S at 1100°C ( $v = 1$ mV/s)	90
<b>Figure 4.4</b>	Micrographs of Ni-30Cr alloy after 24 h of immersion in NC3S at 1100°C with magnification of (a) 500x and (b) 1000x	93
<b>Figure 4.5</b>	Anodic polarisation curves of pure Cr and Ni-30Cr in NC3S at 1100°C after ~ 40 min of immersion (a) comparison of pure Cr and Ni-30Cr alloy (b) anodic polarisation curve of Ni-30Cr alloy	94
<b>Figure 4.6</b>	Trends of current density as a function of potential plots of $\text{Cr}^{\text{II}}/\text{Cr}^0$ and $\text{Si}^{\text{IV}}/\text{Si}^0$ redox couples in the case of pure Cr and Ni-30Cr samples	95
<b>Figure 4.7</b>	Cross section of preoxidised Ni-30Cr alloy after 24 h of immersion in NC3S at 1100°C (a) 200x magnification (b) 2000x magnification	99
<b>Figure 4.8</b>	Evolution of corrosion potential ( $E_{\text{corr}}$ ) and polarisation resistance ( $R_p$ ) of (a) preoxidised pure Cr (b) preoxidised Ni-30Cr alloy during the immersion in NC3S at 1100°C	100
<b>Figure 4.9</b>	Cross section of preoxidised Ni-30Cr alloy after 5 h of immersion in NC3S at 1100°C with (a) 200x magnification (b) 2000x magnification	103
<b>Figure 4.10</b>	Anodic polarisation curves for both non-preoxidised and preoxidised Ni-30Cr alloy after 24 h of immersion in NC3S at 1100°C	103
<b>Figure 4.11</b>	Cross section of preoxidised Ni-30Cr after 24 h of immersion in NC3S at 1150°C (a) region with chromium oxide (b) region with no oxide	104

<b>Figure 4.12</b>	The corrosion potentials ( $E_{\text{corr}}$ ) (a) and polarisation resistance ( $R_p$ ) (b) of preoxidised Ni-30Cr alloy in NC3S at 1100°C and 1150°C	106
<b>Figure 4.13</b>	Anodic polarisation curves of preoxidised Ni-30Cr alloy after 24 h of immersion in NC3S at 1100°C and 1150°C	106
<b>Figure 4.14</b>	Measurement of (a) $E_{\text{corr}}$ and (b) $R_p$ of preoxidised pure Cr during the 24 h of immersion in N1.5S, N2S, N3S, N3.5S and NC3S at 1050°C	110
<b>Figure 4.15</b>	The values of $E_{\text{corr}}$ and $R_p$ of the preoxidised pure Cr after 24 h of immersion in binary melts ( $\text{Na}_2\text{O}-x\text{SiO}_2$ ; $x = 1.5, 2, 3$ and $3.5$ ) and ternary melt (NC3S) at 1050°C, reported as a function of (a) optical basicity ( $\Lambda_{\text{th}}$ ) and (b) activity of $\text{Na}_2\text{O}$ ( $p_a(\text{Na}_2\text{O})$ )	110
<b>Figure 4.16</b>	Metal/glass interface of pure Cr which has been preoxidised in air at 1050°C for 2 h, after 24 h immersion in (a) N1.5S (b) N2S and (c) NC3S at 1050°C	112
<b>Figure 4.17</b>	Thickness of the $\text{Cr}_2\text{O}_3$ layer on the preoxidised Cr samples after 24 h of immersion in N1.5S, N2S and NC3S at 1050°C as a function of Cr content measured near the glass/oxide layer interface	114
<b>Figure 4.18</b>	Micrographs of Ni-30Cr alloy after 24 h of immersion in (a) NC3S and (b) NC6S at 1100°C	116
<b>Figure 4.19</b>	Anodic polarisation curves of non-preoxidised Ni-30Cr in the three different glasses at 1100°C	117
<b>Figure 4.20</b>	Interface metal/glass of pure Cr which has been preoxidised in air at 1050°C for 2 h, after immersion in N1.5S	120
<b>Figure 4.21</b>	Micrographs of preoxidised Ni-30Cr after 24 h immersion at 1100°C in (a) NC3S and (b) NC6S	121

<b>Figure 4.22</b>	Thickness of the Cr <sub>2</sub> O <sub>3</sub> layer on the preoxidised Cr samples after 24 h of immersion in N1.5S, N2S and NC3S at 1050°C as a function of Cr content measured near the glass/oxide layer interface	122
<b>Figure 4.23</b>	Micrographs of NiAl after 24 h of immersion in NC3S at 1100°C with magnification of (a) 200x, (b) 500x and (c) 1000x	126
<b>Figure 4.24</b>	Micrographs of Ni-8Al-28Cr after 24 h of immersion in NC3S at 1100°C with magnification of (a) 100x – Secondary Electrons, (b) 500x – Back Scattered Electrons, (c) 2000x – Back Scattered Electrons and (d) 2000x - Back Scattered Electrons	128
<b>Figure 4.25</b>	The concentration profile of the metal elements in the glass for (a) NiAl (bulk) and (b) Ni-8Al-28Cr after 24 h of immersion in NC3S at 1100°C	129
<b>Figure 4.26</b>	The concentration profiles of the (a) Glass elements and (b) Metal elements in the alloy for NiAl (bulk) after 24 h of immersion in NC3S at 1100°C. The plots in (c) represent the enlargement of the concentration profile in (b) for the distance of 100 µm from the surface of alloy/glass	130
<b>Figure 4.27</b>	The concentration profiles of the (a) Glass elements and (b) Metal elements in the alloy for Ni-8Al-28Cr after 24 h of immersion in NC3S at 1100°C	131
<b>Figure 4.28</b>	Corrosion potentials ( $E_{\text{corr}}$ ) and polarisation resistance ( $R_p$ ) of (a) NiAl (cemented) and (b) Ni-8Al-28Cr in NC3S at 1100°C	132
<b>Figure 4.29</b>	Anodic polarisation curves of (a) NiAl (cemented) and (b) Ni-8Al-28Cr after ~ 20 min of immersion in NC3S at 1100°C	133

<b>Figure 4.30</b>	Micrographs of preoxidised NiAl (cemented) (24 h in air at 1100°C) after 2 h of immersion in NC3S at 1100°C with magnification of (a) 200x and (b) 1000x	136
<b>Figure 4.31</b>	The concentration profile of (a) Glass element and (b) Metal elements in the alloy for preoxidised NiAl (cemented) (24 h in air at 1100°C) after 2 h of immersion in NC3S at 1100°C	136
<b>Figure 4.32</b>	Micrographs of preoxidised Ni-8Al-28Cr (24 h in air at 1100°C) after 2 h of immersion in NC3S at 1100°C with magnification of (a) 500x and (b) 1000x	137
<b>Figure 4.33</b>	The concentration profile of metal elements in the glass for preoxidised Ni-8Al-28Cr (24 h in air at 1100°C) after 2 h of immersion in NC3S at 1100°C	138
<b>Figure 4.34</b>	The concentration profile of (a) Glass element and (b) Metal elements in the alloy for preoxidised Ni-8Al-28Cr (24 h in air at 1100°C) after 2 h of immersion in NC3S at 1100°C	139
<b>Figure 4.35</b>	Corrosion potentials ( $E_{\text{corr}}$ ) and polarisation resistance ( $R_p$ ) of (a) preoxidised (2 h in air at 1100°C) Ni-8Al-28Cr, (b) preoxidised Ni-8Al-28Cr and NiAl (24 h in air at 1100°C) after 2 h of immersion in NC3S at 1100°C. Plots in (c) represent the enlargement of the first hour of immersion in graph (b)	140
<b>Figure 5.1</b>	Cross section of a sample showing the analysed areas	147
<b>Figure 5.2</b>	Plots of distribution of dissolved Cr (at.%) as a function of time in NC5S at 1300°C under oxidising atmosphere (air). The dotted lines are guides to the eyes	148

<b>Figure 5.3</b>	Distribution of Cr <sub>2</sub> O <sub>3</sub> grains in NC5S at 1300°C under oxidising atmosphere (air) after 1 h of experimental duration	149
<b>Figure 5.4</b>	Schematic of dissolution mechanism of Cr <sub>2</sub> O <sub>3</sub> in molten glass under oxidising condition (air) for a short run duration	150
<b>Figure 5.5</b>	Distribution of Cr <sub>2</sub> O <sub>3</sub> grains as a function of time in NC5S at 1300°C under oxidising atmosphere (air) after (a) 9 h, (b) 24 h and (c) 48 h of experimental duration	151
<b>Figure 5.6</b>	Schematic of dissolution mechanism of Cr <sub>2</sub> O <sub>3</sub> in molten glass under oxidising condition (air) for a long experimental duration	152
<b>Figure 5.7</b>	Plot of 2Si/Na ratio as a function of experimental duration at 1300°C under oxidising atmosphere (air). Theoretical ratio is in dotted line	153
<b>Figure 5.8</b>	Plots of the distribution of dissolved Cr (at.%) as a function of time in NC5S at 1300°C under reducing atmosphere (Fe/FeO). The dotted lines are guides to the eyes	154
<b>Figure 5.9</b>	Distribution of Cr <sub>2</sub> O <sub>3</sub> grains in NC5S as a function of time at 1300°C under reducing atmosphere (Fe/FeO) after 1 h of experimental duration	155
<b>Figure 5.10</b>	Schematic of dissolution mechanism of Cr <sub>2</sub> O <sub>3</sub> in molten glass under reducing condition (Fe/FeO). (a) Short experimental duration (b) Optical observation	156
<b>Figure 5.11</b>	Distribution of Cr <sub>2</sub> O <sub>3</sub> grains as a function of time in NC5S at 1300°C under reducing atmosphere (Fe/FeO) after (a) 9 h, (b) 24 h and (c) 48 h of experimental duration	158

<b>Figure 5.12</b>	Plot of 2Si/Na ratio as a function of experimental duration for NC5S at 1300°C under reducing atmosphere (Fe/FeO). Theoretical ratio is in dotted line	159
<b>Figure 5.13</b>	Plots of (a) distribution of dissolved Cr (at.%) and (b) evolution of 2Si/Na ratio as a function of time in NC6S at 1200°C under oxidising atmosphere (air). The dotted lines in (a) are guides to the eyes whereas the dotted line in (b) is the theoretical ratio	160
<b>Figure 5.14</b>	Plots of (a) distribution of dissolved Cr (at.%) and (b) evolution of 2Si/Na ratio as a function of time in NC6S at 1300°C under oxidising atmosphere (air). The dotted lines in (a) are guides to the eyes whereas the dotted line in (b) is the theoretical ratio	161
<b>Figure 5.15</b>	Micrographs of the samples of NC6S + Cr <sub>2</sub> O <sub>3</sub> which were subjected to (a) 24 h and (b) 48 h of heat treatments under oxidising condition (air) at 1300°C	162
<b>Figure 5.16</b>	Plots of (a) distribution of dissolved Cr (at.%) and (b) evolution of 2Si/Na ratio as a function of time in NC6S at 1200°C under reducing atmosphere (Fe/FeO). The dotted lines in (a) are guides to the eyes whereas the dotted line in (b) is the theoretical ratio	163
<b>Figure 5.17</b>	Plots of (a) distribution of dissolved Cr (at.%) and (b) evolution of 2Si/Na ratio as a function of time in NC6S at 1300°C under reducing atmosphere (Fe/FeO). The dotted lines in (a) are guides to the eyes whereas the dotted line in (b) is the theoretical ratio	164
<b>Figure 5.18</b>	Micrographs of the samples of NC6S + Cr <sub>2</sub> O <sub>3</sub> which were subjected to (a) 24 h and (c) 48 h of heat treatments under reducing condition (Fe/FeO) at 1300°C	165

<b>Figure 5.19</b>	Plots of (a) distribution of dissolved Cr (at.%) and (b) evolution of 2Si/Na ratio as a function of time in NC3S and NC6S at 1300°C under oxidising atmosphere (air). The dotted lines in (a) are guides to the eyes whereas the dotted lines in (b) are the theoretical ratio	167
<b>Figure 5.20</b>	Plots of (a) distribution of dissolved Cr (at.%) and (b) evolution of 2Si/Na ratio as a function of time in NC3S at 1300°C under oxidising atmosphere (air). The dotted lines in (a) are guides to the eyes whereas the dotted line in (b) is the theoretical ratio	169
<b>Figure 5.21</b>	Plots of distribution of dissolved Cr (at.%) as a function of time in three different melts at 1200°C under oxidising atmosphere (air). The dotted lines are guides to the eyes	170
<b>Figure 5.22</b>	Plot of 2Si/Na ratio as a function of experimental duration at 1200°C under oxidising atmosphere (air) for three different melts. Theoretical ratios are in dotted line	171
<b>Figure 5.23</b>	Plots of distribution of dissolved Cr (at.%) as a function of time in (a) 0.5C, (b) N3S and (c) NC6S at 1200°C under oxidising atmosphere (air). The dotted lines are guides to the eyes	172
<b>Figure 5.24</b>	Correlation of the Cr solubility in NC3S with temperature (T = 1200°C, 1300°C and 1350°C) for different $fO_2$	180
<b>Figure 5.25</b>	The plots of Cr solubility as a function of oxygen fugacity for two different temperatures and two different compositions. The dotted lines are guides to the eyes	182
<b>Figure 5.26</b>	The variation of total dissolved Cr as a function of (a) 2Si/Na ratio and (b) theoretical optical basicity ( $\Lambda_{th}$ ) for different $fO_2$ at 1200°C. The lines are guides to the eyes	185

<b>Figure 5.27</b>	The evolution of total dissolved Cr as a function of optical basicity for soda-lime silicate melt (NCxS) and soda silicate melt (NxS) for four different $fO_2$ at 1200°C	187
<b>Figure 5.28</b>	The evolution of total dissolved Cr as a function of activity of Na <sub>2</sub> O ( $a_{Na_2O}$ ) for soda-lime silicate melt (NCxS) and soda silicate melt (NxS) for different $fO_2$ at 1200°C	188
<b>Figure 5.29</b>	Calculated viscosity for soda silicate (NxS) and soda-lime silicate (NCxS) melts as a function of temperature (°C)	190
<b>Figure 5.30</b>	Cr species solubility representation as a function of $\log fO_2$ (a) The total dissolved Cr in glass melt; (b) The Cr <sup>III</sup> species contribution; (c) The Cr <sup>II</sup> species contribution; (d) The Cr <sup>VI</sup> species contribution	192
<b>Figure 5.31</b>	Variation of $\log (Cr^n/Cr^{III})$ as a function of $\log fO_2$ in the glass NC3S at T = 1200°C	194
<b>Figure 5.32</b>	The concentration profile of Cr in the melts measured on Ni-30Cr alloy after immersion at 1100°C for 24 hours in NC3S and NC6S and at 1150°C for 24 hours for NC3S	198



## LIST OF SYMBOLS

<b>Symbols</b>	<b>Descriptions</b>
$E_a$	Activation energy
$a$	Activity
$\beta_a$	Anodic kinetics constant
$\beta_c$	Cathodic kinetics constant
$I_{\text{corr}}$	Corrosion current density
$E_{\text{corr}}$	Corrosion potential
$V_{\text{thickness loss}}$	Corrosion rate (thickness loss)
$V_{\text{corr}}$	Corrosion rate (Stern-Geary)
$\rho$	Density
$\emptyset$	Diameter
$k'_1$	Linear constant
$D^*$	Network oxygen diffusion coefficient
$D$	Oxygen diffusion coefficient
$fO_2$	Oxygen fugacity

$k'_p$	Parabolic constant
$R_p$	Polarisation resistance
$S$	Surface area
$T$	Temperature
$t$	Time
$\Lambda_{th}$	Theoretical optical basicity
$\eta$	Viscosity

## LIST OF ABBREVIATIONS

BSE	Backscattered electron
DTA	Differential thermal analysis
EPMA	Electron probe micro-analysis
SEM	Scanning electron microscope
SE	Secondary electron
NCxS	$\text{Na}_2\text{O}-\text{CaO}-x\text{SiO}_2$ (Soda-lime silicate)
NxS	$\text{Na}_2\text{O}-x\text{SiO}_2$ (Soda silicate)
TGA	Thermogravimetric analysis
UV-Vis	Ultraviolet-visible spectroscopy
XRD	X-ray diffraction analysis

**KAJIAN SIFAT-SIFAT REDOKS DAN ASID-BES KACA SODA-KAPUR  
SILIKAT: APLIKASI UNTUK KAKISAN BERSUHU TINGGI ALOI  
BERASASKAN NIKEL DAN BAHAN-BAHAN SERAMIK**

**ABSTRAK**

Sifat kakisan aloi-aloi pembentuk kromia ( $\text{Cr}_2\text{O}_3$ ) dan alumina ( $\text{Al}_2\text{O}_3$ ) dalam leburan soda-kapur silikat dikaji dengan menggunakan teknik 'rendaman' yang disertakan dengan pengukuran elektrokimia. Gabungan kedua-dua teknik tersebut membawa kepada penentuan aspek-aspek umum kakisan oleh kaca terlebur serta tindakbalas redoks dan kinetik yang mengawal proses kakisan. Keputusan eksperimen mendedahkan bahawa  $\text{Al}_2\text{O}_3$  tidak dapat memberikan perlindungan terhadap kakisan oleh kaca terlebur oleh kerana ia mempunyai keterlarutan yang tinggi di dalam leburan tersebut. Walau bagaimanapun, aloi pembentuk  $\text{Cr}_2\text{O}_3$  dapat menahan terhadap kakisan oleh kaca terlebur jika aloi tersebut telah dilakukan rawatan pra-pengoksidaan dalam udara sebelum rendaman. Oleh kerana ketahanan lapisan  $\text{Cr}_2\text{O}_3$  berkait dengan persaingan antara pembentukan oksida dan keterlarutannya dalam leburan, maka ciri-ciri fizikokimia  $\text{Cr}_2\text{O}_3$  dalam kaca leburan seterusnya dikaji dengan mendalam bagi memahami pengaruh parameter yang berbeza terhadap had keterlarutan  $\text{Cr}_2\text{O}_3$ . Kajian telah dijalankan dengan mengambil kira pengaruh suhu ( $T$ ), fugasiti oksigen ( $f\text{O}_2$ ) dan komposisi kaca terhadap kebolehlarutan  $\text{Cr}_2\text{O}_3$  dalam leburan. Kajian awal kinetik mendedahkan bahawa masa untuk mencapai keseimbangan berbeza bagi parameter tersebut. Walau bagaimanapun, masa keseimbangan kompromi dipilih untuk memuaskan semua masalah yang dihadapi. Kajian termodinamik menunjukkan bahawa pengaruh  $T$  dan  $f\text{O}_2$  terhadap keterlarutan  $\text{Cr}_2\text{O}_3$  dalam leburan soda-kapur silikat ternari ( $\text{Na}_2\text{O-CaO-}$

$x\text{SiO}_2$ ) kelihatan koheren dengan leburan binari ( $\text{Na}_2\text{O}-x\text{SiO}_2$ ). Walau bagaimanapun, keterlarutan  $\text{Cr}_2\text{O}_3$  dalam leburan ternari adalah lebih rendah daripada leburan binari. Nilai keterlarutan Cr dalam  $\text{Na}_2\text{O}-\text{CaO}-x\text{SiO}_2$  ( $x = 3, 4, 5$  and  $6$ ) untuk suhu yang berbeza ( $T = 1200^\circ\text{C}, 1300^\circ\text{C}$  and  $1350^\circ\text{C}$ ) dan fugasiti oksigen yang berbeza ( $-12 \leq \log f_{\text{O}_2} \leq -0.6$ ) berada antara 0.23 at.% hingga 1.09 at.%. Pengaruh kebesan dikaji terhadap leburan ternari dan binari dengan mengambil kira kebesan optik teori ( $\Lambda_{\text{th}}$ ) dan aktiviti  $\text{Na}_2\text{O}$ . Nisbah redoks ( $\text{Cr}^{\text{II}}/\text{Cr}^{\text{III}}$  and  $\text{Cr}^{\text{VI}}/\text{Cr}^{\text{III}}$ ) ditentukan melalui penghalusan matematik. Perbandingan dengan keputusan yang telah diperolehi dalam leburan binari dan penyimpangan dari nilai teori yang dijangkakan apabila melibatkan spesies kromium, menimbulkan andaian mengenai peranan yang dimainkan oleh CaO dalam mempengaruhi tindak balas yang melibatkan spesies daripada pasangan  $\text{O}^{2-}/\text{O}_2$ .

# **STUDY OF THE REDOX AND ACID-BASE PROPERTIES OF SODA-LIME SILICATE GLASS: APPLICATION TO THE HIGH TEMPERATURE CORROSION OF NICKEL-BASED ALLOYS AND CERAMIC MATERIALS**

## **ABSTRACT**

The corrosion behaviour of chromia ( $\text{Cr}_2\text{O}_3$ ) and alumina ( $\text{Al}_2\text{O}_3$ ) forming alloys in soda-lime silicate melts was studied by using 'raw immersion' technique which was coupled with electrochemical measurements. The combination of both techniques leads to the determination of the general aspects of the corrosion by the molten glass as well as the redox reactions and the kinetics that rule the corrosion process. The results revealed that  $\text{Al}_2\text{O}_3$  is not able to provide protection against corrosion by molten glass since it has a high dissolution in the melt. However  $\text{Cr}_2\text{O}_3$  forming alloy could resist against corrosion by molten glass if the alloy was subjected to a preoxidation treatment in air before the immersion. As the durability of the  $\text{Cr}_2\text{O}_3$  layer is linked to the competition between the oxide growth and its dissolution in the melt, the physicochemical properties of  $\text{Cr}_2\text{O}_3$  in molten glasses were then thoroughly studied in order to understand the influence of different parameters on the limit of  $\text{Cr}_2\text{O}_3$  solubility. The works were conducted by taking into account the influence of temperatures ( $T$ ), oxygen fugacities ( $f\text{O}_2$ ) and the glass compositions on the solubility of  $\text{Cr}_2\text{O}_3$  in the melts. The preliminary kinetics study revealed that the time to reach equilibrium varies with the parameters ( $T$ ,  $f\text{O}_2$  and glass compositions). However, a compromising equilibrium time was chosen in order to satisfy all the problems encountered. The thermodynamic study showed that the influence of  $T$  and  $f\text{O}_2$  on the  $\text{Cr}_2\text{O}_3$  solubility in ternary soda-lime silicate melts ( $\text{Na}_2\text{O}-\text{CaO}-x\text{SiO}_2$ ) seems to be in coherence with the results in binary melts ( $\text{Na}_2\text{O}-$

$x\text{SiO}_2$ ). Nevertheless, the  $\text{Cr}_2\text{O}_3$  solubility in ternary melts is lower than in binary melts. The Cr solubility values in  $\text{Na}_2\text{O-CaO-}x\text{SiO}_2$  ( $x = 3, 4, 5$  and  $6$ ) for different temperatures ( $T = 1200^\circ\text{C}, 1300^\circ\text{C}$  and  $1350^\circ\text{C}$ ) and different oxygen fugacity ( $-12 \leq \log f_{\text{O}_2} \leq -0.6$ ) lie between 0.23 at.% to 1.09 at.%. The influence of basicity was studied in these ternary and binary melts by taking into account the theoretical optical basicity ( $\Lambda_{\text{th}}$ ) and the activity of  $\text{Na}_2\text{O}$  ( $a_{\text{Na}_2\text{O}}$ ). The redox ratios ( $\text{Cr}^{\text{II}}/\text{Cr}^{\text{III}}$  and  $\text{Cr}^{\text{VI}}/\text{Cr}^{\text{III}}$ ) were determined through a mathematical refinement. The comparison with the results obtained in binary melts and the deviation from the theoretical values expected when speciation of Cr is involved, induce the assumption of the role played by CaO in influencing the reactions involving species from  $\text{O}^{2-}/\text{O}_2$  couple.

# **ETUDE DES PROPRIÉTÉS ET ACIDO-BASIQUE DE VERRE SODO-CALCIQUE: APPLICATION À LA CORROSION HAUTE TEMPÉRATURE D'ALLIAGES BASE NICKEL ET DE MATÉRIAUX CÉRAMIQUES**

## **RÉSUMÉ**

Le comportement en corrosion d'alliage chromine ( $\text{Cr}_2\text{O}_3$ ) et alumine ( $\text{Al}_2\text{O}_3$ ) formeurs dans des verres sodo-calciques à haute température a été étudié en couplant des techniques électrochimiques avec la caractérisation post-mortem des matériaux immergés dans le milieu fondu. Les mécanismes réactionnels de la corrosion par ce type de milieu ont ainsi pu être abordés, de même que les aspects cinétiques. Les résultats ont montré que l'alumine n'était pas capable de protéger les alliages contre la corrosion, dans la mesure où sa solubilité dans le verre est particulièrement importante. Cependant, les alliages chromine formeurs ont montré de bonne propriété de résistance à la corrosion, dans la mesure où ceux-ci ont préalablement subi un traitement de pré-oxydation. Lors de l'immersion, une compétition entre la croissance de la couche de chromine et sa dissolution dans le verre s'installe, régissant ainsi la durée de vie de la couche d'oxyde protectrice. En conséquence, une attention particulière a été portée sur la physico-chimie de la chromine en milieu verre fondu. La solubilité de la chromine a donc été étudiée afin de comprendre l'influence des paramètres température ( $T$ ), fugacité en oxygène ( $f\text{O}_2$ ) et composition du verre. Une étude cinétique préliminaire a permis de mettre en évidence l'influence de ses paramètres sur les mécanismes et le temps de mise à l'équilibre. D'un point de vue thermodynamique, l'influence des paramètres  $T$  et  $f\text{O}_2$  sur la solubilité du chrome dans des verres ternaires  $\text{Na}_2\text{O-CaO-xSiO}_2$  est cohérente avec les études antérieurement menées sur des verres binaires  $\text{Na}_2\text{O-xSiO}_2$ . Néanmoins, la solubilité



de la chromine est nettement plus faible dans le cas des verres ternaires. Les valeurs de la solubilité de Cr dans  $\text{Na}_2\text{O-CaO-xSiO}_2$  ( $x = 3, 4, 5$  and  $6$ ) pour différentes températures ( $T = 1200^\circ\text{C}, 1300^\circ\text{C}$  and  $1350^\circ\text{C}$ ) et différente fugacité en oxygène ( $-12 \leq \log f_{\text{O}_2} \leq -0.6$ ) se situent entre 0.23 at.% à 1.09 at.%. L'influence de la basicité a été parallèlement étudiée dans les verres binaires et ternaires, en prenant en compte la basicité optique théorique ( $\Lambda_{\text{th}}$ ) et l'activité en oxyde de sodium ( $a_{\text{Na}_2\text{O}}$ ). Les rapports redox ( $\text{Cr}^{\text{II}}/\text{Cr}^{\text{III}}$  et  $(\text{Cr}^{\text{VI}}/\text{Cr}^{\text{III}})$ ) ont été déterminées suite à un affinement mathématique. La comparaison avec les résultats obtenus dans le cas des verres binaires ainsi que de grandes différences observées par rapport aux résultats théoriques dans le cas où la spéciation du chrome intervient laissent penser que l'oxyde de calcium CaO a une influence dans les réactions impliquant les espèces du couple  $\text{O}_2/\text{O}^{2-}$ .

## CHAPTER 1

### INTRODUCTION

In high temperature industries, most of the metallic parts normally consist of nickel-based alloys with high chromium and aluminium contents, which can lead to the formation of chromia,  $\text{Cr}_2\text{O}_3$  and alumina,  $\text{Al}_2\text{O}_3$  when in contact with air atmosphere at high temperature. These two oxides are very well known to provide good protection against oxidation as they usually form homogeneous and protective layers on the alloys.

The biggest challenge faced by the production of glass is related to the lifetime of the glass processing equipments which are in contact with molten glass. These equipments are expected to have the ability to withstand harsh environments and thus to resist against high temperature corrosion since they are normally consist of chromia ( $\text{Cr}_2\text{O}_3$ ) forming alloys with chromium mass content ranging from 25 to 30 wt.%. However, the stability of these alloys in molten glasses, which is mainly governed by the dissolution of the protective chromia in the melts, is one of the crucial factors that determine the lifetime of these metallic parts.

During the last 20 years, the team "Surface et Interface : Réactivité Chimique des Matériaux" has been focusing on the corrosion of different materials in molten glass media. In a first approach, electrochemical methods has been used in order to characterise the corrosion behaviour of the metals/alloys in molten glass. The ability of the alloys to build a protective chromia layer has been emphasized as the best candidates for long term corrosion resistance in molten glass media. As a

consequence, the works have been continued by a more specific study devoted to the behaviour of chromia in molten silicates. In this work, a focus has been given on the characterisation of the basicity of the media; a crucial property of the glass which gives a profound influence on the behaviour of chromia in the melt. A previous PhD work led by Sandra Abdelouhab has contributed to the development of the *in situ* measurement of the activity of the strong base, sodium oxide ( $\text{Na}_2\text{O}$ ). This work proved the profound effect of different parameters on the corrosivity of molten silicates, *i.e.* temperature, oxygen fugacity and basicity. As a continuity, a second PhD work performed by Hichem Khedim, dealt with the study of the solubility of chromia in simple binary glasses ( $\text{Na}_2\text{O}$ - $x\text{SiO}_2$  system). Through this work a specific device has been developed, allowing the control of the temperature, oxygen fugacity and glass composition parameters independently.

The work proposed here is an extension of the study of the solubility of chromium in glasses whose basic composition is similar to the most common industrial glass. In this present work, an introduction of the calcium oxide ( $\text{CaO}$ ) to the simple binary glass has been taken into account. The aim is to have a closer investigation towards a well-known corrosive system *i.e.* CMAS ( $\text{CaO}$ - $\text{MgO}$ - $\text{Al}_2\text{O}_3$ - $\text{SiO}_2$ ), which is directly involved in the corrosion of TBC (Thermal Barriers Coatings). In addition,  $\text{CaO}$  which is a basic oxide also behaves as a network modifier as  $\text{Na}_2\text{O}$ . Therefore, it is necessary to evaluate the effect of  $\text{CaO}$  addition to binary glassy matrix  $\text{Na}_2\text{O}$ - $x\text{SiO}_2$  on the physicochemical properties of the ternary system.

The present work is a continuity of the previous studies in the binary soda silicate  $\text{Na}_2\text{O-xSiO}_2$  melts. The objectives of this work are (i) to evaluate the performances of chromia forming and alumina forming alloys in simplified soda silicate and soda-lime silicates in order to compare the ability of these oxides to give protection against corrosion in molten glasses (ii) to extend the knowledge of the physicochemical properties of chromia in simplified molten silicates of the  $\text{Na}_2\text{O-xSiO}_2$  system by an addition of a second network modifier which is the basic oxide CaO. The manuscript is organised as follows:

Firstly, a literature review is proposed in the second chapter. A description of the molten glass media is given, in terms of structure, acid base properties, and redox properties. Then, the state of art on the corrosion of metals and alloys in molten glass is presented. Chromia and alumina forming alloys are thus emphasised. Then, a part deals with the previous studies devoted to the behaviour of chromia in silicate melts is presented in the final part of this chapter.

The materials and experimental methods used in this work are presented in the third chapter. The characterisation of the raw materials, alloys and glasses used in this study is detailed in Appendices. The specific electrochemical characterisation of the corrosion in molten media is detailed herein. The electrodes used in molten glass at high temperature are an adaptation from the methods used in aqueous media. The reactor allowing the independent control of temperature, oxygen fugacity and glass composition which has been developed in a previous oxide solubility study is also described in this chapter.

The fourth chapter is devoted to the determination of the corrosion of (i) chromia forming and (ii) alumina forming Ni-based simplified alloys in different types of silicate melts. A 'Raw immersion' test followed by a thorough observation of the samples give informations about the general aspects of the corrosion by the molten glass (surface morphology, glass penetration, thickness loss, oxide thickness, etc.). Correlation is then made with the electrochemical measurements, which allows an access to further information on the redox reactions and the kinetics ruling the corrosion process. An accurate comparison is made between chromia and alumina about their ability to give an efficient protection against glass corrosion.

Since the chromia has the ability to provide protection to the alloys due to its low solubility in molten glass, its physicochemical properties are then detailed in the fifth chapter. Firstly, the dissolution kinetics of chromia in different conditions (*i.e.* temperature, oxygen fugacity, melt composition) are thoroughly studied herein. The aim is to choose the best duration of heat treatment in order to be as close as possible to the equilibrium, thus allowing a pertinent thermodynamic study. The mechanisms which are strongly correlated to the diffusion of oxygen species in the melt are also discussed.

The last part deals with the solubility of chromia in the ternary system  $\text{Na}_2\text{O}-\text{CaO}-x\text{SiO}_2$ . The influences of temperature and oxygen fugacity are first observed, in the same way as in the previous study performed in binary melts. Then, a specific attention is paid on the role played by CaO in the melts, and its influence on the physicochemical properties of the Cr oxo-complex species.

## CHAPTER 2

### LITERATURE REVIEW

#### Introduction

This chapter is devoted to a brief description of the physicochemical properties behind the word 'glass' as well as the corrosion phenomena occurring in molten glass. The prerequisite for this attempt is to have an understanding of the structure and the components of the glass which will be discussed in the first part. Secondly, the theoretical and experimental of the concept of acid-base in molten glass as well as the redox reactions in the melts will be discussed thoroughly through a synthetic review of the state of art of many previous studies. The phenomena of corrosion of metals and alloys in molten glasses will be described in the next part. As the protection of the alloys in molten glasses is related to the nature and stability of the oxide layer formed at the interface alloy/glass, hence the physicochemical behaviour of some important oxides in molten glasses will be presented in the final part.

#### 2.1. General aspects of glass

The silicate glass has become a high-tech material with numerous applications in various fields including industry (aeronautic, power generation, glass fibre elaboration, etc.), architecture, arts and as very recently, in waste management's with the use of glass matrices for the stabilisation and the storage of nuclear waste. The term 'glass' brings many contradictions among scientists whether it should be classified as a solid or as a liquid. However, by considering the definition behind the term 'glass', it actually refers to a state of matter, usually produced when a viscous

molten material is cooled rapidly to below its glass transition temperature, with insufficient time for a regular crystal lattice to form. Being neither a liquid nor a solid, but sharing the qualities of both, glass possesses its own state of matter which is called an amorphous solid. Unlike crystals, glass does not have a sharp melting point and does not cleave in preferred directions. Glass also shows elasticity like crystalline solids. Thus, instead of describing the glass by its definition, it is more appropriate to define it by considering the physicochemical properties of the glass itself which strongly depend on its structure.

### **2.1.1. Formation and structure of silicate network**

Unlike crystal (Figure 2.1(a)), glass is a three-dimensional network of atoms forming a solid that lacks periodicity or ordered pattern (Figure 2.1(b)). Random atomic arrangement as would appear in a sodium silicate glass has been shown schematically in Figure 2.1(c). In this case, a  $\text{Si}^{4+}$  acts as the building block of the glass network which is known as a network-forming cation (NWF)<sup>1</sup>. The four positive charges of the silicon ion tend to form bonds with four oxygen atoms, forming  $\text{SiO}_4$  tetrahedra *i.e.* four-sided pyramidal shapes, connected to each other at the corners. An oxygen atom that connects two tetrahedra is known as bridging oxygen while the oxygen atom which joins to only one silicon atom is called a non-bridging oxygen. In the example of sodium silicate glass (Figure 2.1(c)), a univalent sodium ion ( $\text{Na}^+$ ) occupies an interstice adjacent to the  $\text{SiO}_4$  tetrahedra in order to balance the remaining negative charge. The role played by  $\text{Na}^+$  in the silicate network will be discussed thoroughly in the next part. This corner-sharing tetrahedral structure achieves a liquid-like randomness rather than a crystalline regularity

because of the random value of the Si-O-Si angle. Furthermore, there are twist angles arising between two connected tetrahedra.

Glass consists of network formers, network modifiers and intermediates<sup>1,2</sup>. In order to predict the oxides that tend to form glasses, Zachariasen<sup>3</sup> has proposed four rules for glass formation:

- No oxygen atom may be linked to more than two cations.
- The cation coordination number is small: 3 or 4.
- Oxygen polyhedra share corners, not edges or faces.
- For 3D networks, at least three corners must be shared.

- $\bullet$   $\text{Si}^{4+}$
- $\circ$   $\text{O}^{2-}$
- $\textcircled{\text{hatched}}$   $\text{Na}^+$

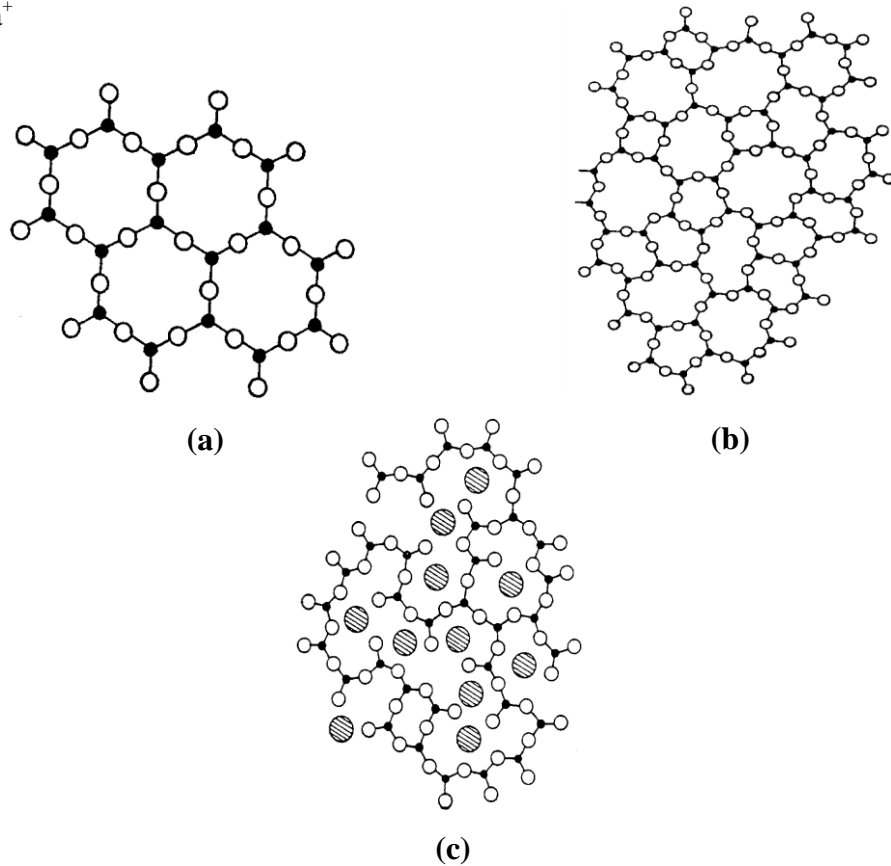


**Figure 2.1:** Schematic of two dimensions of (a) crystalline quartz (b) amorphous silica (c) soda silicate glass. The fourth Si-O bond is placed perpendicularly to the plane of the figure<sup>1</sup>



Apart from Zachariassen<sup>3</sup>, Sun<sup>4</sup> has also introduced a correlation between the strength of the interatomic bonds and the ability of the material to form a glass. The classification of the substances with regard to their glass-forming ability has become the most important contribution of Sun's single bond criterion. Dietzel<sup>5</sup> has proposed to characterise the ability of the cations to form a network with oxygen ions by the Coulomb's force of attraction. It is known as the 'field strength' and can be described by the following equation:

$$A = \frac{Z_c}{(r_c + r_o)^2} \quad (2.1)$$

where  $Z_c$  is the cation valence,  $r_c$  and  $r_o$  are the cation and  $O^{2-}$  radii respectively and expressed in Å. The values of the field strength ( $A$ ) for various cations are presented in Table 2.1. The value of  $A > 1.0$  represents the cations of the network formers whereas  $A < 0.35$  corresponds to the cations of the network modifiers.

**Table 2.1:** The field strength of various cations<sup>5</sup>

Elements	$Z_c$	$r_c$	$A = \frac{Z_c}{(r_c + r_o)^2}$	
P	5	0.31	1.710	Cation formers
V	5	0.49	1.400	
Si	4	0.40	1.235	
B	3	0.25	1.102	
Sb	5	0.74	1.092	
Ge	4	0.53	1.074	
Ti	4	0.74	0.873	Cation intermediates
Al	3	0.53	0.805	
Zr	4	0.86	0.783	
Be	2	0.41	0.610	
Mg	2	0.86	0.392	
Zn	2	0.88	0.385	

**Table 2.1:** Continued<sup>5</sup>

Elements	$Z_c$	$r_c$	$A = \frac{Z_c}{(r_c + r_o)^2}$	
Ca	2	1.14	0.310	Cation modifiers
Pb	2	1.33	0.268	
Li	1	0.90	0.189	
Na	1	1.16	0.153	
K	1	1.52	0.117	

**2.1.1.1. Network formers**

According to Zachariasen<sup>3</sup>, the cations which have the coordination number of 3 or 4 could readily form glasses and are commonly known as 'network formers' as they provide the backbone in other mixed-oxide glasses. However, this rule is not applicable for all cases. For example,  $Al_2O_3$  is not able to form glass when the oxide is alone since the charges are not sufficient to form a stable polyhedron with four oxygen. The examples of network formers are  $B_2O_3$ ,  $SiO_2$ ,  $P_2O_5$  and  $GeO_2$ .

**2.1.1.2. Network modifiers**

Alkali and alkaline-earth elements such as Li, Na, K, Ca and Mg play a role as a network modifiers in the glass network<sup>2</sup>. A network former such as  $SiO_2$  is well-known for its high melting temperature which lies between  $1600^\circ C$  -  $1725^\circ C$ . At this temperature, the liquid is very viscous, making the processing of the glass difficult. Since the network modifiers have the ability to break up the covalent bonds between the network formers and the anions, a network modifier such as  $Na_2O$  which is known as a 'flux' is always added to the network formers such as  $SiO_2$  in order to decrease the melting temperature of pure  $SiO_2$  and also the viscosity of the melts.

There are two important effects by an addition of  $\text{Na}_2\text{O}$  to the network. Firstly, every  $\text{Na}_2\text{O}$  molecule will disrupt the network and will cause the formation of two groups of  $\text{Si}-\text{O}^-\text{Na}^+$  (Figure 2.2). The oxides that have the ability to modify the network are called 'network modifiers' since they can transform the bridging oxygen (the oxygen that links to two cation formers) into non-bridging oxygen (oxygen which links to only one cation former). The breaking of the Si-O bonding lowers the viscosity of the melt, thus facilitating the fusion process. Secondly, an alkali oxide such as  $\text{Na}_2\text{O}$  has the ability to lower the liquidus temperature of the melt, thus limiting the risk of devitrification phenomenon.

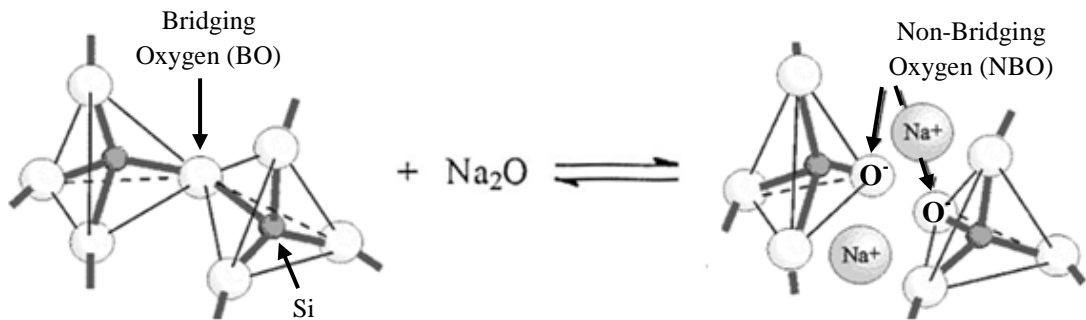


**Figure 2.2:** Schematic of the breaking of Si-O bonding by introducing a  $\text{Na}_2\text{O}$  molecule in the silicate network<sup>2</sup>

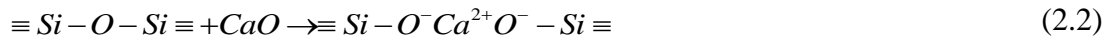
### 2.1.1.3. Intermediates

The intermediate oxides are less clearly defined compared to the network formers and network modifiers. The intermediates may act as network formers or network modifiers depending on the glass compositions. The oxides such as  $\text{Al}_2\text{O}_3$ ,  $\text{BeO}$ ,  $\text{MgO}$  and  $\text{ZnO}$  are examples of the intermediates<sup>2</sup>. The intermediate cations create a slightly covalent binding with the  $\text{O}^{2-}$  anions. The coordination tendency of these ions is insufficient to establish a three-dimensional network. Since the intermediates can establish a bond with two or three oxygen ions, the addition of intermediates to a silica glass does not lead to a complete breaking up of the

polyhedra network. The presence of the intermediates suppresses the tendency of the glass melt to form crystals during cooling.

#### 2.1.1.4. The role of CaO

CaO is an alkaline-earth oxide playing a role as a glass modifier since it also breaks the Si-O bonding in the network<sup>2</sup>. The introduction of CaO into the network could be described by the following equation:



An addition of CaO to the network leads to the creation of two non-bridging oxygen. It can also decrease the viscosity of the molten glass but the effect is more moderate compared to the addition of alkali oxide. Furthermore, the effect of an addition of alkaline-earth oxide on the decreasing the liquidus temperature of the silicate network is less significant compared to the alkali oxide since the alkaline-earth oxides are more refractory compared to the alkali oxide.

In the case of soda-lime silicate glass, an addition of CaO will break the bridging of Si-O-Si bonds between silicate tetrahedron, thus decreasing the average silicate chain length. However, the electronic charge of calcium ion which is higher than sodium ion makes the  $[SiO_4]^{4-}$  to be more easily associated with  $Ca^{2+}$  ions compared to the monovalent cation. Therefore, the  $Na^+$  ions are potentially freer in the Ca-bearing system relative to the sodium-silica binary. According to Abdelouhab *et al.*<sup>6</sup>, the increased number of non-bridging oxygen in the Ca-bearing system ( $Na_2O-CaO-xSiO_2$ ) may lead to an increase in the  $Na_2O$  activity relative to that

observed in the equivalent  $\text{Na}_2\text{O-xSiO}_2$  melt. Addition of CaO to a binary alkali silicate glass is known to increase its durability<sup>1</sup>. They are chemically durable against water and acid and have fairly good weathering resistance. However, soda-lime silicate glass has high thermal expansion, thus prone to thermal shock failure.

#### **2.1.1.5. The role of $\text{Al}_2\text{O}_3$**

$\text{Al}_2\text{O}_3$  will never form glass itself but acts like a glass former or modifier if combined with other oxides<sup>2</sup>. Therefore  $\text{Al}_2\text{O}_3$  is classified as an intermediate in the glass network. By introducing in the pure  $\text{SiO}_2$ ,  $\text{Al}^{3+}$  has the coordination number of VI, thus playing a role as a network modifier.  $\text{Al}_2\text{O}_3$  has the ability to be a network former in the alkali-containing glasses when  $\text{Al}^{3+}$  substitutes  $\text{Si}^{4+}$  in the network. Every  $\text{Al}_2\text{O}_3$  introduced in the melt will remove a pair of non-bridging oxygen (associated with two  $\text{Na}^+$  which must neutralise the two  $[\text{AlO}_4]^{5-}$  tetrahedra) which leads to an increase of the glass viscosity due to the formation of aluminate tetrahedra<sup>7</sup>. However, the structural role of the  $\text{Al}^{3+}$  in alkali silicate glasses depends on the aluminium concentration and the temperature of the melts<sup>8</sup>.

#### **2.1.2. Acid-base properties in glass melts**

As in the aqueous media, the acid-base properties play an important role in the molten glass for the theoretical understanding of the nature of some physicochemical processes in glass-forming melts and slags, as well as for applied tasks, *e.g.* the prediction of the process tendencies and design of the materials with necessary characteristics. Acid-base properties of the glass also show a significant influence on the corrosion of metal/alloys by molten glasses<sup>9-11</sup>. A large number of studies have been performed in order to reveal the theories of acid-base in the molten

glass<sup>12-19</sup> as well as to determine a scale to distinguish the acidity or basicity of the melts.

#### **2.1.2.1. Acid-base concepts in glass melts**

The Brönsted-Lowry<sup>12,13</sup> theory provides a broader definition of acids and bases in a protonic solvent. According to this theory:

- An acid is defined as a species which has the tendency to yield a proton.
- A base is a substance that can accept a proton.

The Brönsted-Lowry theory still does not present the full generalisation of acid-base phenomena. This theory does take into account the experimental fact that there are many substances besides the hydroxyl ion which exhibit typical basic properties, but fails to recognise complementary data with regard to acids. Therefore, the proton transfer acid-base theory has practically no application in glass.

As a contrary, Lewis<sup>14</sup> theory considers acid-base functions and related processes independently of the solvent. According to Lewis:

- An acid is any species that is capable of accepting a pair of electrons to form a covalent bond by sharing with the electron donor.
- A base is any species that can donate a pair of electrons to form a covalent bond with the acid.

Although it can overcome many difficulties in aqueous solution, the application of Lewis theory in glass melt raises doubt since there is a close relationship between acid-base function and oxidation-reaction in the molten glass. Even though both acids and oxidising agents tend to accept electrons, however the acid accepts electron

pairs and forms coordinate covalent bonds whereas the oxidising agent keeps the electrons to itself.

The concept of acid-base in molten oxides was first introduced by Lux<sup>15</sup> in 1939. His definition can be represented by the following equation:



The concept of Lux was developed by Flood and Förland in 1947<sup>16</sup> and remains actual up to the present time. Flood and Förland have summarised that the acid-base in an oxide system is characterised by the transfer of an  $\text{O}^{2-}$  ion from one state of polarisation to another. The degree of basicity of an oxide is determined by the ability of oxygen atoms to give up electrons. The basicity is greater when the  $\text{O}^{2-}$  ion is unaffected by surrounding cations. As a summary of Lux and Flood theory in the case of molten oxides and molten salts, the exchange of  $\text{O}^{2-}$  ions between the base and the acid can be assimilated to the exchange of electrons in the Lewis theory. A strong base is capable of combining with electron acceptor which is known as oxoacid. The species resulting from these combinations are called oxobase. For example:

- Metal oxides ( $\text{Na}_2\text{O}$ ,  $\text{BaO}$ ,  $\text{Al}_2\text{O}_3$ , ...) are bases and metal cations ( $\text{Na}^+$ ,  $\text{Ba}^{2+}$ ,  $\text{AlO}^+$ , ...) are conjugate acids.
- Oxoanions ( $\text{SiO}_3^{2-}$ ,  $\text{SO}_4^{2-}$ ,  $\text{CO}_3^{2-}$ , ...) are bases and the oxides ( $\text{SiO}_2$ ,  $\text{SO}_3$ ,  $\text{CO}_2$ , ...) are conjugate acids.

These couples react according to the following equilibrium:



The equilibrium constant, K:

$$K = \frac{a_{acid} \times a_{\text{O}^{2-}}}{a_{base}} \quad (2.5)$$

will be a measure of the strength of the acid-base pair.

By analogy with the aqueous solution where the  $\text{H}^+$  ion activity allows to establish an acidity scale ( $\text{pH} = -\log a(\text{H}^+)$ ), the activity of  $\text{O}^{2-}$  ions has been used as a basicity indicator in the molten glass<sup>15,17,18</sup> or in a medium where the  $\text{O}^{2-}$  ions exist as free ions according to the following equation:

$$\text{pO}^{2-} = -\log a(\text{O}^{2-}) \quad (2.6)$$

where  $a(\text{O}^{2-})$  is the activity of the oxide ions in the medium. It is noteworthy that the  $\text{pO}^{2-}$  scale works in the reverse direction as compared with the pH scale in protonic solvents. In contrary with the case of aqueous solution where the standard state of  $\text{H}^+$  ion can be defined precisely (water is a universal solvent), no standard state can be defined for molten glass because the composition of the solvent varies from one glass to another. Furthermore, the basicity of the oxide melts depends on the force of the ionic bonding between  $\text{O}^{2-}$  and the cation modifier<sup>1</sup>. The basicity increases with the increase in ionic radii of the alkali ions and alkaline-earth ions. Therefore, the basicity increases by descending the column of alkali and alkaline-earth elements and decreases by going through the group of alkali and alkaline-earth in the periodic



table. Since the terms "acidity" and "basicity" are determined via  $O^{2-}$  activity, both characteristics become indiscernible. Therefore, the boundary dividing "acid" and "base" in melts is a problem of standardisation and quantitative of  $pO^{2-}$  measurement<sup>19</sup>.

#### **2.1.2.2. Evaluation of acid-base properties in molten glass**

The acid-base properties in the molten glass have been defined through theoretical and calculation models by several authors. Moreover, some efforts have been made in order to measure the basicity of the molten glass through *ex situ* and *in situ* measurements.

##### *(a) Theoretical models of calculation*

Many studies have been devoted to develop theoretical models of calculation of acid-base properties in molten glass in order to quantify the activity of oxide ion ( $O^{2-}$ ) and the activity of non-bridging oxygen as a function of glass composition.

##### ➤ *Model of Sun*

In 1948, Sun<sup>20</sup> estimates the strength of cation-oxygen bonding by the formation enthalpy of the glass. The strength of cation-oxygen bonding depends on the dissociation energy of the oxides in the molten glass and the coordination of oxygen with the cation. According to this model, an acid is a network former which has a high electron affinity. Cameron<sup>21</sup> has proposed to calculate the glass basicity based on the value of oxides basicity from Sun<sup>20</sup>. The basicity of boric oxide has been randomly chosen as the origin of the scale. The glass basicity is proportional to the basic number « B »:

$$a(O^{2-}) = Cst \times B \quad (2.7)$$

where

$$B = 119 - \left( \frac{A_{Sun(oxideA)} \times \%mol}{100} + \frac{A_{Sun(oxideB)} \times \%mol}{100} + \dots \right) \quad (2.8)$$

The basicity value of oxides ( $A_{Sun}$ ) which has been proposed by Sun is compiled in Table 2.2:

**Table 2.2:** The values of  $A_{Sun}$  allowing to determine the acid-base properties of the glass<sup>20</sup>

Oxides	$A_{Sun}$
K <sub>2</sub> O	13
Na <sub>2</sub> O	20
BaO	33
Li <sub>2</sub> O	36
MgO	37
PbO	36-39
Al <sub>2</sub> O <sub>3</sub>	53-67
Sb <sub>2</sub> O <sub>3</sub>	68-85
B <sub>2</sub> O <sub>3</sub>	119
As <sub>2</sub> O <sub>3</sub>	70-87
SiO <sub>2</sub>	106

➤ *Model of Sanderson*

Sanderson<sup>22-25</sup> has proposed a model to calculate the acid-base properties in the glass by considering a magnitude ( $x$ ) which is attributed to the size of an atomic electron density. The magnitude  $x$  can be related to the Pauling electronegativity ( $\chi$ ) by the following equation:

$$x = \frac{\sqrt{\chi} - 0.77}{0.21} \quad (2.9)$$

For an oxide  $M_mO_n$ , the value  $x$  can be calculated according to the following equation:

$$xM_mO_n = \left[ (x_M)^m (x_O)^n \right]^{\frac{1}{m+n}} \quad (2.10)$$

Thus, the acidity/basicity of the glass  $A_{\text{glass}}$  can be determined by the following equation:

$$A_{\text{glass}} = (x_1^{N_1} \times x_2^{N_2} \times \dots \times x_n^{N_n} \times 5.02)^{\frac{1}{(N_1+N_2+\dots+N_m+1)}} \quad (2.11)$$

where  $x_i$  is the Sanderson electronegativity of element  $i$ , and  $N_i$  is the total number of oxygen in the system.

➤ *Model of Toop and Samis*

In 1962, Toop and Samis<sup>26</sup> have proposed the existence of three different forms of oxygen:

- The bridging oxygen which links to two silicon atoms ( $O^0$ ).
- The non-bridging oxygen which links to one silicon atom ( $O^-$ ).
- The free oxide ion ( $O^{2-}$ ).

It is possible to develop an equilibrium between these three forms of oxygen and thus to derive the equilibrium constant as expressed by the following equations:



$$K = \frac{a(O^{2-}) \times a(O^0)}{a(O^-)^2} \quad (2.13)$$

The value of  $K$  is constant for a given temperature and it represents the characteristic of cations present in the molten glass. In this equation, Toop and Samis have replaced the activities of the components by their concentrations, hence specified the equilibrium proportions for each form of presented oxygen. For a molten oxide with a composition  $nM_2O-(1-n)SiO_2$ , the number of moles of oxygen atoms bonding to silicon atoms  $4(1-n)$  can be written as the following equation:

$$2N(O^0) + N(O^-) = 4(1-n) \quad (2.14)$$

where  $N(O^0)$  and  $N(O^-)$  are the number of bridging and non-bridging oxygens. Thus, the following equation can be derived:

$$N(O^0) = \frac{4(1-n) - N(O^-)}{2} \quad (2.15)$$

The number of free oxide ions can be represented by the following equation:

$$N(O^{2-}) = n - \frac{N(O^-)}{2} \quad (2.16)$$

Since the reaction of one mole of oxide modifier with silica gives rise to two moles of non-bridging oxygen, the equilibrium constant between the three forms of oxygen can be written in assimilating the activities with their concentrations:

$$K = \frac{N(O^{2-}) \times N(O^0)}{N(O^-)^2} \quad (2.17)$$

By replacing the  $N(O^{2-})$  and  $N(O^0)$  by Eq. 2.16 and Eq. 2.15 respectively, the following equation can be derived:

$$K = \frac{[(4-4n) - N(O^-)] \times [2n - N(O^-)]}{4N(O^-)^2} \quad (2.18)$$

Eq. 2.18 can be simplified by the following equation:

$$(4K-1) \times N(O^-)^2 + (4-2n)N(O^-) + 8(n^2 - n) = 0 \quad (2.19)$$

The resolution of this equation for various values of equilibrium constants and for different stoichiometries allows the determination of the distribution of the three forms of oxygen present in the melt under the considered environment. However, Konakov<sup>19</sup> has pointed that the states of  $O^0$  in  $SiO_2$  and the formed silicates, as well as  $O^-$  in these silicates, are indiscernible. Therefore, the Toop and Samis model was rather limited and could not be used for an adequate description of the acid-base interactions in real oxide melts. However, the approach by Toop and Samis was partly used in many known models<sup>1,27,28</sup>.

#### *(b) Experimental measurements*

Due to the importance of the knowledge of acid-base properties in the molten glass and the difficulties in predicting it, many authors have developed some techniques in order to measure experimentally the acid-base properties in molten glass.

➤ *Gaseous solubility*

The relative basicity of molten glass can be evaluated experimentally by the solubility of certain gases ( $\text{H}_2\text{O}^{29,30}$ ,  $\text{CO}_2^{31-33}$ ,  $\text{SO}_2^{34}$ ) which dissolve in the glass network. The solubility of the gas will increase at any constant pressure of oxygen as the oxygen ion activity in the melt increases. Since the oxygen ion activity is related to the basicity of the melt, an increase in the solubility of the gas can be used as an indicator of an increase in the basicity of the melt.

➤ *Transition metal ions as acid-base indicators*

Paul and Douglas<sup>35-37</sup> have proposed a method by using transition metal ions as acid-base indicators in glass. The transition metals which have been introduced in molten glass behave like a Lewis acid and interact with the free oxide ions in order to form an oxocomplex. The possibility of using transition metal ions as indicators in silicate glasses is due to the fact that the coordination symmetry of these ions changes with the basicity of the melt. Due to their incompletely filled inner shell, the oxocomplex formed can be studied thoroughly by spectroscopic and magnetic measurements. The cations that are widely used in this method are  $\text{Ni}^{\text{II}}$ <sup>35</sup>,  $\text{Co}^{\text{II}}$ <sup>36</sup> and  $\text{Cr}^{\text{VI}}$ <sup>37</sup>. In the case of  $\text{Ni}^{\text{II}}$  and  $\text{Co}^{\text{II}}$ , a change of coordination from octahedral symmetry to tetrahedral symmetry with increasing basicity can be determined by spectroscopic measurements since the optical absorption characteristics of octahedral and tetrahedral are distinctly different.

➤ *Transpiration method*

Since basicity of the melt links to the content of network modifiers in the glass, the transpiration method is dedicated to determining the activity of sodium

oxide ( $a(\text{Na}_2\text{O})$ ) which plays a role as a network modifier by measuring the vapour pressure of the distillation gas of the molten oxides. Rego *et al.*<sup>38</sup> have used the transpiration technique to measure the vapour pressures of Na above the stirred  $\text{Na}_2\text{O-xSiO}_2$  melts which are in equilibrium with graphite crucible and CO. The experiments have been performed at 1300°C and 1400°C for silica-rich melts under a system pressure of one atmosphere. Under these reducing conditions, the expected reaction is:



The equilibrium constant for the above reaction allows the determination of the activity of  $\text{Na}_2\text{O}$  in the silicate melts according to the following equation:

$$\log(a_{\text{Na}_2\text{O}}) = \log[(p_{\text{Na}})^2 \times p_{\text{CO}}] - \log K \quad (2.21)$$

The quantity  $\log [(p_{\text{Na}})^2 \times p_{\text{CO}}]$ , which is related to the  $a(\text{Na}_2\text{O})$  is plotted as a function of compositions for each two temperatures. The second-order curve fits give an access to the  $\log K$  values, thereby allowing the determination of  $a\text{Na}_2\text{O}$  by the following equations:

at 1300°C,

$$\log a_{\text{Na}_2\text{O}} = -9.86 + 6.22X_{\text{Na}_2\text{O}} + 6.75(X_{\text{Na}_2\text{O}})^2 \quad (2.22)$$

and at 1400°C,

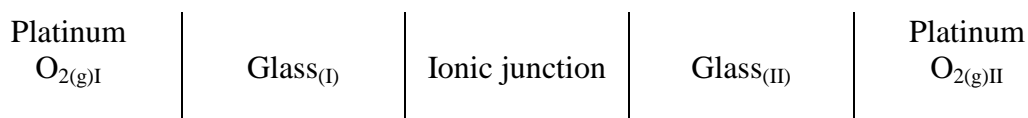
$$\log a_{\text{Na}_2\text{O}} = -9.01 + 2.44X_{\text{Na}_2\text{O}} + 11.8(X_{\text{Na}_2\text{O}})^2 \quad (2.23)$$

where  $X_{\text{Na}_2\text{O}}$  is the mole fraction of  $\text{Na}_2\text{O}$  in the glass. An extension of this work, using an encapsulation technique to study the  $\text{Na}_2\text{O-CaO-SiO}_2$  and  $\text{Na}_2\text{O-MgO-SiO}_2$  systems and some synthetic blast-furnace slags have been described by Rego *et al.*<sup>39</sup> in another work.

➤ *EMF measurement*

The oxygen ion activity of two melts can be compared by measuring the difference of the electrochemical potential of oxygen in the melts. The only direct method by which oxygen ion activities can be compared independently without interference from other reactions is through an electromotive force measurement (EMF)<sup>1</sup>. This method requires the use of a reversible oxygen electrode immersed in molten glass. Thus, a platinum electrode which has been flushed by air is the best candidate for this type of application. It is also necessary to provide a bridge between the glasses being compared which has negligible junction potential. The basicity of the molten glass has been determined by measuring the different potentials between the working melt (studied melt) and the reference melt (melt with well-known basicity). The junction between the two glasses is ensured either by a  $\beta$  alumina<sup>6,40-42</sup> refractory or by a direct contact between these two glasses through a small diameter of orifice<sup>43,44</sup>.

The potential generated by the electrochemical cell of type:



is given by the following equation if  $\text{O}_2(\text{Pt})_{\text{I}} = \text{O}_2(\text{Pt})_{\text{II}}$ :



$$\Delta E = \frac{-RT}{2F} \times \ln \frac{a(\text{Na}_2\text{O})_{(II)}}{a(\text{Na}_2\text{O})_{(I)}} \quad (2.24)$$

where Glass<sub>(I)</sub> is the reference glass and the Glass<sub>(II)</sub> is the working glass. The Eq. 2.24 can be expressed as:

$$\ln a(\text{Na}_2\text{O})_{II} = \ln a(\text{Na}_2\text{O})_I - \frac{2F\Delta E}{RT} \quad (2.25)$$

This method allows a direct access to the relative basicity of a molten glass. Unlike the other methods which have been discussed before, the EMF measurement allows the determination of the basicity of the molten glass without modifying the solvent by an addition of gas or an indicator. Furthermore, a wide range of glass compositions can be studied using this technique especially for a higher acidity melt where the conventional method such as gas dissolution may not give an accurate result.

The activity of Na<sub>2</sub>O in Na<sub>2</sub>O-SiO<sub>2</sub> and Na<sub>2</sub>O-CaO-SiO<sub>2</sub> systems has been measured by Neudorf and Elliott<sup>40</sup> by using this method. It has been demonstrated that an addition of CaO to the binary Na<sub>2</sub>O-SiO melt causes an increase in the activity of Na<sub>2</sub>O. The experimental activity data seems to have a good agreement with the values calculated using Richardson ideal mixing model<sup>40</sup>.

The EMF measurement has been also applied by Abdelouhab *et al.*<sup>6</sup> in order to quantify the activity of Na<sub>2</sub>O in a series of sodium-bearing silicate melts at high temperature. Abdelouhab has tried to make a comparison between the log a(Na<sub>2</sub>O) obtained via EMF measurement and the calculated basicity using theoretical model